technology based on modern IT. *CIS Iron and Steel Review*. 2014. No. 1. pp. 44–49.
5. Pehterev S. V., Ivin Yu. A., Nikolaev O. A., Kazyatin K. B., Semenov P. S. Production of high-strength reinforced bar steel for Russian Railways. *Chernye metally*. 2013. No. 6. pp. 27–32.
6. Chabby L. Simulation of microstructure and mechanical properties in section rolling. *Chernye metally*. 2017. No. 9. pp. 57–62.
7. Kopylov I. V., Volkov K. V., Romadin A. Yu. Features of the ways of longitudinal slitting in rolling of rebars. *Kalibrovochnoe byuro*. 2013. No. 2. pp. 5-14. (available at: http://www.passdesign.ru).
8. Starkov N. V., Bobarykin Yu. L. Perfomance critetia slitting-process. *Lityo i metallurgiya*. 2016. No. (1) 82. pp. 61–65.
9. Mroz S., Szota P., Dyja H., Numerical Modeling of Rolling Process Using Longitudinal Slitting Passes. *AISTech Proceedings*. 2005. pp. 775–783.
10. Stefanik A., Mroz S., Szota P., Dyja H. Determination of slitting criterion parameter during the multi slit rolling process. *AIP Conference Proceedings*. 2007. pp. 1231–1236.
11. Starkov N. V., Bobarikin Yu. L. Choosing the Slitting Method and the Profile of the Slitting Rolls for Rolling and Slitting. *Metallurgist*. 2015. Vol. 59. Iss. 5–6. pp. 390–395.
12. Wisselink H. H., Huetink J. 3D FEM simulation of stationary metal forming processes with applications to slitting and rolling. *Journal of Materials Processing Technology*. 2004. No. 148. pp. 328–341.
13. Zhuchkov S. M., Lokhmatov A. P., Andrianov N. V., Matochkin V. A. Rolling-Slitting with the Use of Undriven Slitting Equipment: Theory and Practice. Pan-Press. Ukraine-Belarus. 2007.
14. Efimov O. Yu., Chinokalov V. Ya., Kopylov I. V., Fastykovskii A. R., Makhrin A. N. Employing rolling and separation technology in the 250-1 mill. *Steel in Translation*. 2008. Vol. 38. No. 8. pp. 671–673.
15. Efimov O. Yu., Fastykovskii A. R., Chinokalov V. Ya., Kopylov I. V. Introduction of a splitting operation in rolling on a continuous small-bar mill. *Steel in Translation*. 2008. Vol. 38. No. 4. pp. 327–328.

UDC 621.778.24 DOI: http://dx.doi.org/10.17580/cisisr.2018.01.05

SPRINGBACK COEFFICIENT OF ROUND STEEL BEAM UNDER ELASTOPLASTIC TORSION

V. N. Shinkin[1]

[1] *National University of Science and Technology "MISIS" (Moscow, Russia)*
E-mail: shinkin-korolev@yandex.ru

AUTHOR'S INFO

V. N. Shinkin, Dr. Sci. (Phys.-Math.), Prof.

Key words:

Key words: steel straight round beam, torsion of round beam, torque, tangential stress, cross-section of round beam, springback coefficient, elastoplastic deformation, continuous medium.

ABSTRACT

After the elastoplastic deformation of the metal structures and the metal products (for example, after a torsion, a bending, a compression, a stretching, the complex types of deformations), these bodies change their shape and partially springback. At the same time, the residual stresses arise in the bodies. Under the appropriate external conditions (for example, when the temperature changes), these stresses can lead to a significant distortion of the bodies' shape (adopted after deformation) and even destroy these bodies. To estimate the residual shape of the round steel beam, which it takes after the mechanical deformation (the forming), it is necessary to know the springback coefficient of the round beam at the torsion. At the torsion of a round steel beam, the torques (the torsional moments, the twisting moments) also appear in the beam. This moments are connected with the tangential stresses in its cross-section. The maximum of the tangential stresses occur on the surface of the round beam and can lead to the destruction of the metal beam. However, even at very strong elastoplastic torsion around the symmetry axis of the beam, the tangential stress in the center of the cross-section of the round beam is zero and the elastic zone in the beam's cross-section exists. Therefore, the destruction of the round steel beam and the defects of its metal under the torsion always start at the beam's surface. The magnitude of the tangential stresses and angular deformations, their distribution along the cross-section of the round beam are always associated with the torque of the external forces. The greater the torque, the greater the tangential stresses and angular deformations. In this paper we have obtained the springback coefficient and the torques of the straight round beam under a torsion for an elastoplastic medium with a linear hardening, depending on the beam's radius, the shear modulus, the yield strength and the hardening modulus of beam's material. The research results can be used in the metallurgical and machine-building factories.

1. Introduction

We consider a straight beam with a circular cross-section with the radius R. Further, we will assume that the material of the beam under the elastoplastic torsion has a linear hardening.

Let τ and γ be a tangential stress and a shear angle; G, L and τ_y be the shear modulus, the hardening modulus and the yield strength at shear of beam's material [1–39]. The diagram of tangential stresses of the beam for the medium with linear hardening at shear is shown in **fig. 1**.

In the field of elastic deformations, the tangential stresses obey the Hooke's law at shear

$$\tau = G\gamma.$$

In the field of material's hardening (the elastoplastic torsion), the dependence of the tangential stress τ on the shear angle γ has the form

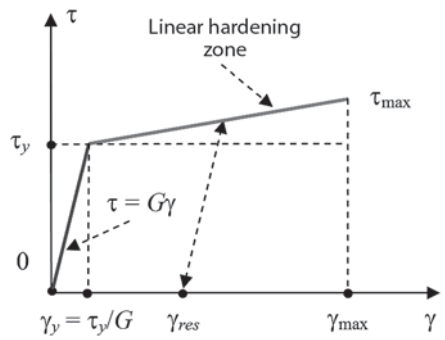

Fig. 1. The dependence of the tangential stress on the twist angle

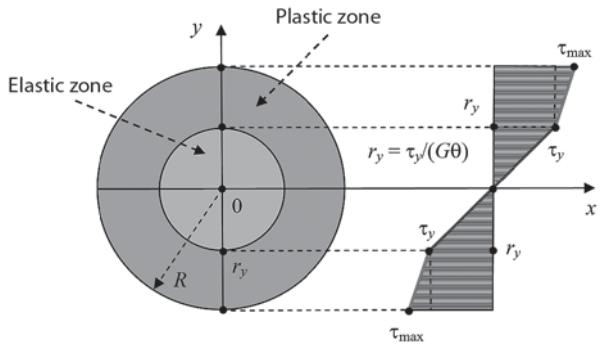

Fig. 2. The epure of the tangential stresses in the cross section of the round beam

$$\tau = \tau_y + L\left(\gamma - \gamma_y\right) = \tau_y + L\left(\gamma - \frac{\tau_y}{G}\right),$$

$$\gamma_y = \frac{\tau_y}{G}, \quad \tau_{max} = \tau_y + L\left(\gamma_{max} - \frac{\tau_y}{G}\right).$$

At a torsion of the straight beam with a circular cross-section, the maximum tangential stresses are observed on the beam's surface. The epure of the tangential stress in the cross-section of the round beam is shown in **fig. 2**.

Under the strength condition by Huber – Mises (the energy theory of strength), we have [1–4, 12, 13]

$$\tau_y = \frac{\sigma_y}{\sqrt{3}} \approx 0.58\,\sigma_y,$$

but under the strength condition by Tresca – Saint-Venant (the theory of maximum tangential stresses), we have

$$\tau_y = \frac{\sigma_y}{2} \approx 0.5\,\sigma_y.$$

2. Torsion of round beam

Let $\varphi(z)$ be the twist angle of the cross-section of the round beam. The relative twist angle $\theta(z)$ of the beam's cross-section is equal

$$\theta = \theta(z) = \frac{d\varphi}{dz}.$$

The cross-section of the round beam under the torsion is divided into two zones — the elastic zone and the plastic zone. The value r_y which determines the boundary of these zones is found from the equations

$$\tau_y = G\gamma_y = Gr_y\theta, \quad r_y = \frac{\tau_y}{G\theta}, \quad \frac{\tau_y}{Gr_y\theta} = 1.$$

If the torque and the relative twist angle increase, the elastic area of the beam's cross-section decreases.

In the elastic area of the beam's cross-section we have [8–11, 19–21]

$$\tau = G\gamma = Gr\theta,$$

but in the plastic area of the beam's cross-section we have

$$\tau = \tau_y + L\left(\gamma - \gamma_y\right) = \tau_y + L\left(\gamma - \frac{\tau_y}{G}\right) = \tau_y + L\left(r\theta - \frac{\tau_y}{G}\right),$$

$$\tau_{max} = \tau_y + L\left(R\theta - \frac{\tau_y}{G}\right).$$

The relative twist angle of the beam, at which for the first time the tangential stress on the beam's surface equals to the yield strength at shear τ_y, we find from the equations

$$r_y = R, \quad \tau_y = GR\theta_y, \quad \theta_y = \frac{\tau_y}{GR}, \quad \frac{\tau_y}{GR\theta_y} = 1.$$

According to the strength condition by Huber – Mises (the energy strength theory), we have

$$\tau_y = \frac{\sigma_y}{\sqrt{3}}, \quad \theta_y = \frac{\tau_y}{GR} = \frac{\sigma_y}{\sqrt{3}GR},$$

but according to the strength condition by Tresca – Saint-Venant (the theory of maximum tangential stresses), we have

$$\tau_y = \frac{\sigma_y}{2}, \quad \theta_y = \frac{\tau_y}{GR} = \frac{\sigma_y}{2GR}.$$

3. Torque

Under the elastoplastic torsion, the torque M in the cross-section of the beam is equal to

$$M = \frac{1}{2}\pi\theta\left[(G-L)\left(\frac{\tau_y}{G\theta}\right)^4 + LR^4\right] +$$

$$+ \frac{2}{3}\pi\tau_y\left(1 - \frac{L}{G}\right)\left(R^3 - \left(\frac{\tau_y}{G\theta}\right)^3\right).$$

Under $L = 0$ (the tangential stress diagram by Prandtl), we obtain

$$M\langle L=0\rangle = \frac{1}{2}\pi\theta\left[G\left(\frac{\tau_y}{G\theta}\right)^4\right] + \frac{2}{3}\pi\tau_y\left(R^3 - \left(\frac{\tau_y}{G\theta}\right)^3\right) =$$

$$= \frac{1}{2}\pi\theta G r_y^{\,4} + \frac{2}{3}\pi\tau_y\left(R^3 - r_y^{\,3}\right) =$$

$$= \frac{1}{2}\pi\tau_y r_y^{\,3} + \frac{2}{3}\pi\tau_y\left(R^3 - r_y^{\,3}\right) =$$

$$= -\frac{1}{6}\pi\tau_y r_y^{\,3} + \frac{2}{3}\pi\tau_y R^3,$$

$$M\langle L=0\rangle = -\frac{1}{6}\pi\tau_y r_y^{\,3} + \frac{4}{6}\pi\tau_y R^3,$$

$$r_y = \sqrt[3]{4R^3 - \frac{6M\langle L=0\rangle}{\pi\tau_y}}.$$

On the other hand, under $L = 0$, the torque is equal to

$$M\langle L=0\rangle = \frac{1}{2}\pi\tau_y\frac{G\theta}{\tau_y}\left(\frac{\tau_y}{G\theta}\right)^4 + \frac{2}{3}\pi\tau_y\left(R^3 - \left(\frac{\tau_y}{G\theta}\right)^3\right) =$$

$$= \frac{1}{6}\pi\tau_y R^3\left[4 - \left(\frac{\tau_y}{GR\theta}\right)^3\right].$$

$$M\langle L=0, \theta=\theta_y\rangle = \frac{1}{2}\pi\tau_y R^3, \quad M\langle L=0, \theta=\infty\rangle = \frac{2}{3}\pi\tau_y R^3.$$

Under $L = 0$, the plastic deformation on the surface of the round beam occurs for the first time when

$$r_y = R = \sqrt[3]{4R^3 - \frac{6M\langle L=0\rangle}{\pi\tau_y}}, \quad M\langle L=0\rangle = \frac{1}{2}\pi\tau_y R^3.$$

Under $L = 0$, the maximum torque is reached at

$$r_y = 0 = \sqrt[3]{4R^3 - \frac{6\max M\langle L=0\rangle}{\pi\tau_y}},$$

$$\max M\langle L=0\rangle = \frac{2}{3}\pi\tau_y R^3.$$

Under $R = r_y$ and $\theta = \theta_y = \tau_y/(GR)$, we obtain

$$M\langle R=r_y, \theta=\theta_y\rangle = \frac{1}{2}\pi\theta_y\left[(G-L)R^4 + LR^4\right] =$$

$$= \frac{1}{2}\pi\theta_y GR^4 = \frac{1}{2}\pi\tau_y R^3.$$

We give the expression for the torque to a dimensionless form

$$\frac{2M}{\pi\tau_y R^3} = \frac{1}{3}\left(1-\frac{L}{G}\right)\left(4-\left(\frac{\tau_y}{GR\theta}\right)^3\right) + \frac{L}{G}\left(\frac{G\theta R}{\tau_y}\right).$$

Under $L = 0$ and $\theta = \theta_y$, we obtain

$$\theta_y = \frac{\tau_y}{GR}, \quad \theta_y R = \frac{\tau_y}{G}, \quad \frac{\tau_y}{GR\theta_y} = 1, \quad \frac{GR\theta_y}{\tau_y} = 1,$$

$$\frac{2M}{\pi\tau_y R^3} = \frac{1}{3}\left(1-\frac{L}{G}\right)\left(4-\left(\frac{\tau_y}{GR\theta}\right)^3\right) + \frac{L}{G}\left(\frac{G\theta R}{\tau_y}\right),$$

$$\frac{2M}{\pi\tau_y R^3} = \frac{1}{3}\left(4-\left(\frac{\tau_y}{GR\theta_y}\right)^3\right) = 1 = \frac{GR\theta_y}{\tau_y},$$

$$\frac{2M}{\pi\tau_y R^3} = 1 = \frac{GR\theta_y}{\tau_y}.$$

Under the pure elastic torsion of the round beam, we have [30, 31, 34, 37–39]

$$I_p = \frac{\pi D^4}{32} = \frac{\pi R^4}{2}, \quad W_p = \frac{\pi D^3}{16} = \frac{\pi R^3}{2},$$

$$\tau_{\max} = \frac{M}{W_p} = \frac{16M}{\pi D^3} = \frac{2M}{\pi R^3} \le \tau_y, \; M \le \frac{1}{2}\pi\tau_y R^3 = \frac{1}{16}\pi\tau_y D^3.$$

Under the pure elastic torsion, the torque M in the cross-section of the beam is equal to

$$M = \frac{1}{2}\pi G\theta R^4,$$

$$\frac{2M}{\pi GR^3} = \theta R = \frac{\tau_y}{G}\frac{GR\theta}{\tau_y}, \quad \frac{2M}{\pi\tau_y R^3} = \frac{GR\theta}{\tau_y}.$$

The dependence $y = 2M/(\pi\tau_y R^3)$ from $x = GR\theta/\tau_y$ is shown in **fig. 3** where

$$y = x - x_{res}, \quad \frac{2M}{\pi\tau_y R^3} = \frac{GR\theta}{\tau_y} - \frac{GR\theta_{res}}{\tau_y} = \frac{GR}{\tau_y}(\theta - \theta_{res}),$$

$$\theta_{res} = \theta - \frac{2M}{\pi GR^4}.$$

4. Springback coefficient under torsion

Under the pure elastic torsion of the straight round beam, the residual relative twist angle is equal to zero ($\theta_{res} = 0$), and the springback coefficient of the straight round beam at torsion is also equal zero ($\beta(\theta) = 0$).

In the basis of determining of the residual relative twist angle θ_{res} after the elastoplastic torsion of the round straight beam, the Genki's theorem about unloading (1924 year) have a place [4, 8, 9, 35–37]: the residual deformatioms are equal to the difference between the true deformations in the elastoplastic body and the deformations which would be created in the body under the assumption of the ideal elasticity of the body's material.

Using the Genki's theorem about unloading, we calculate the springback coefficient $\beta(\theta)$ of the relative twist angle θ_{res} under the torsion of the straight round beam:

$$\theta_{res} = \theta - \frac{2M}{\pi GR^4} = \left(1 - \frac{2M}{\pi GR^4\theta}\right)\theta = \beta(\theta)\theta,$$

$$\beta(\theta) = 1 - \frac{2M}{\pi GR^4\theta} = 1 - \frac{\tau_y}{GR\theta}\left(\frac{2M}{\pi\tau_y R^3}\right) =$$

$$= 1 - \frac{\tau_y}{GR\theta}\left[\frac{1}{3}\left(1-\frac{L}{G}\right)\left(4-\left(\frac{\tau_y}{GR\theta}\right)^3\right) + \frac{L}{G}\left(\frac{G\theta R}{\tau_y}\right)\right],$$

$$\beta(\theta) = \frac{1}{3}\left(1-\frac{L}{G}\right)\left(1-\frac{\tau_y}{GR\theta}\right)^2\left[\left(\frac{\tau_y}{GR\theta}\right)^2 + 2\left(\frac{\tau_y}{GR\theta}\right) + 3\right],$$

$$\theta_{res} = \beta(\theta)\theta,$$

$$\beta\langle\theta=\infty\rangle = 1 - \frac{L}{G}, \quad \beta\left\langle\theta = \theta_{res} = \frac{\tau_s}{GR}\right\rangle = 0.$$

Under $L = 0$ (the tangential stress diagram by Prandtl), we obtain

$$\beta(\theta) = \frac{1}{3}\left(1-\frac{\tau_y}{GR\theta}\right)^2\left[\left(\frac{\tau_y}{GR\theta}\right)^2 + 2\left(\frac{\tau_y}{GR\theta}\right) + 3\right].$$

$$\beta\langle\theta=\infty\rangle = 1, \quad \beta\left\langle\theta = \theta_{res} = \frac{\tau_s}{GR}\right\rangle = 0.$$

The dependence of the springback coefficient β from the relative twist angle θ under $L = 0$ is shown in **fig. 4**.

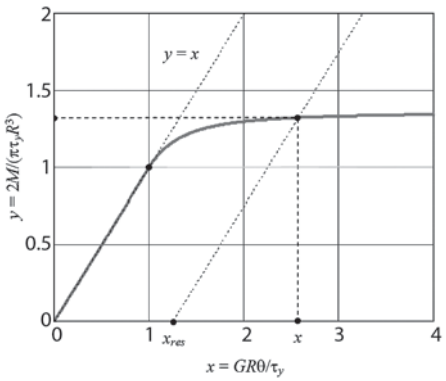

Fig. 3. The dependence of the torque moment from the relative twist angle

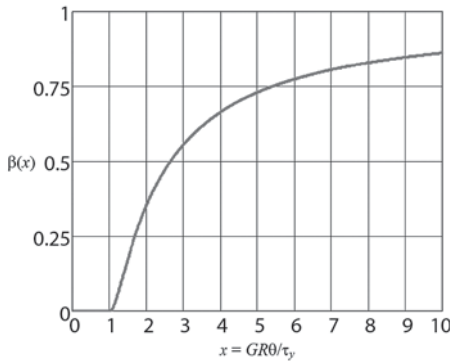

Fig. 4. The dependence of the springback coefficient from the relative twist angle

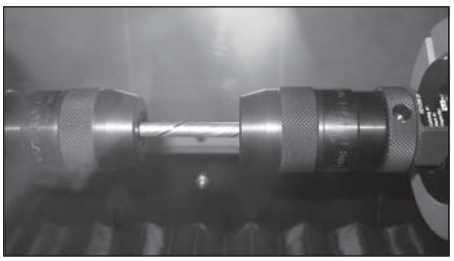

Fig. 5. The torsion of steel wire with a diameter of 5 mm with the help of the collet-chucks by means of the machine Instron 55MT2

Fig. 6. The destruction of the round beam and the loss of stability of the cylindrical shape of the wire's surface under a strong torsion (a violation of the Bernoulli's hypothesis about the plane cross-sections)

The torsion of a piece of steel wire with a diameter of 5 mm on the machine Instron 55MT2 with a maximum torque of 220 N·m and a mass of 2500 N is shown in **fig. 5**. The ends of the wire are clamped with collet-chucks. Before torsion, a straight longitudinal line was applied to the wire's surface with the help of a black marker pen. This line takes a spiral shape during torsion.

The peculiarity of the fracture of a thin long round wire (a diameter up to 5 mm) made of steel, copper and aluminum is its ability to withstand a large plastic deformation (tens of revolutions around the longitudinal axis of symmetry) without completely destroying. Before breaking, thin longitudinal fibers burst on the surface of a thin wire (the surface becomes barbed and rough to the touch), but the initial cylindrical surface of the wire loses its stability and becomes slightly wavy (see **fig. 6**).

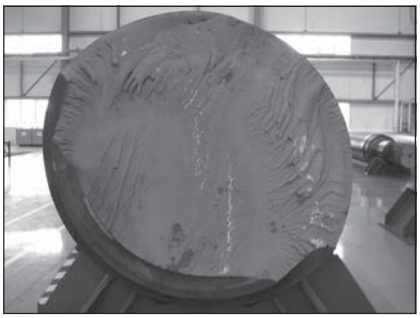

Fig. 7. The destruction of the round steel working roller of 1210×5300 mm by SMS Siemag company on the metallurgical complex mill (MKC-5000)

Destruction of thick steel cylindrical specimens occurs in a different scenario. In an initial stage of torsion of a thick round beam, there are only the tangential stresses in the planes perpendicular to its longitudinal axis. The stress state is a pure shear at all points of the cross-section. On the other hand, there are only normal (main) stresses in the planes located at an angle of 45° to the beam's axis. The normal and tangential stresses are equal in a magnitude to each other, so a destruction of the sample under a torsion can occur from a shear or a break.

Since the shear resistance and the tear resistance for the different materials are different, the destruction of the samples during the torsion test will be different. The destruction of the round beam from the plastic materials (for example, a low-carbon steel) during a torsion is caused by a pure shift and occurs along a cross section of the beam. The destruction of the round beam from the brittle materials (for example, a cast iron) during a torsion occurs due to a separation along the helical surface inclined to the axis of symmetry at an angle of 45°.

The destruction of the round steel working roller of 1210×5300 mm by SMS Siemag company on the metallurgical complex mill (MKC-5000) is shown in **fig. 7**.

5. Conclusions

An analytical expression for the springback coefficient of a round steel beam under an elastoplastic torsion is obtained. The research results can be applied in the metallurgical and machine-building industry under the manufacture of the round beam and armatures, and the metal products made from the round beam and construction armatures [1–39].

REFERENCES

1. Hu J., Marciniak Z., Duncan J. Mechanics of Sheet Metal Forming. Butterworth-Heinemann. 2002. 211 p.
2. Hu P., Ma N., Liu L.-Z., Zhu Y.-G. Theories, methods and numerical technology of sheet metal cold and hot forming. Analysis, simulation and engineering applications. Springer. 2013. 120 p.
3. Frank V. Lecture notes in production engineering. Springer. 2013. 211 p.
4. Calladine C. R. Plasticity for engineers. Theory and applications. Woodhead Publishing. 2000. 328 p.
5. Belskiy S., Mazur I., Lezhnev S., Panin E. Distribution of linear

pressure of thin-sheet rolling across strip width. *Journal of Chemical Technology and Metallurgy*. 2016. Vol. 51. No. 4. pp. 371–378.
6. Belskiy S. M., Yankova S., Chuprov V. B., Bakhaev K. V., Stoyakin A. O. Temperature field of stripes under hot rolling. *Journal of Chemical Technology and Metallurgy*. 2015. Vol. 50. No. 6. pp. 613–616.
7. Belskiy S. M., Yankova S., Mazur I. P., Stoyakin A. O. Influence of the transversal displacements of metal on the camber formation of hot-rolled strip. *Journal of Chemical Technology and Metallurgy*. 2017. Vol. 52. No. 4. pp. 672–678.
8. Chakrabarty J. Theory of plasticity. Butterworth-Heinemann. 2006. 896 p.
9. Chakrabarty J. Applied plasticity. Springer. 2010. 758 p.
10. Klocke F. Manufacturing processes 1. Cutting. Springer. 2011. 506 p.
11. Klocke F. Manufacturing processes 4. Forming. Springer. 2013. 516 p.
12. Shinkin V. N. Calculation of steel sheet's curvature for its flattening in the eight-roller straightening machine. *Chernye Metally*. 2017. No. 2. pp. 46–50.
13. Shinkin V. N. Calculation of bending moments of steel sheet and support reactions under flattening on the eight-roller straightening machine. *Chernye Metally*. 2017. No. 4. pp. 49–53.
14. Mikhailov A. M., Zubarev K. A., Kotel'nikov G. I., Semin A. E., Grigorovich K. V. Vaporization of the components of nickel alloys in a vacuum induction furnace. *Steel in Translation*. 2016. Vol. 46. No. 1. pp. 26–28.
15. Kuznetsov M. S., Yakushev E. V., Kulagin S. A., Kotel'nikov G. I., Semin A. E., Chegeliya R. K. Effect of the charge composition on the nitrogen content in a metal during steelmaking in an ASF using a solid charge. *Russian Metallurgy (Metally)*. 2011. Vol. 2011. No. 12. pp. 1101–1105.
16. Korostelev A. A., Kotelnikov G. I., Semin A. E., Bozheskov A. N. Analysis of HBI effect in charge on technological parameters of EAF melting. *Chernye Metally*. 2017. No. 10. pp. 33–40.
17. Tursunov N. K., Semin A. E., Kotelnikov G. I. Kinetic features of desulphurization process during steel melting in induction crucible furnace. *Chernye Metally*. 2017. No. 5. pp. 23–29.
18. Tursunov N. K., Semin A. E., Sanokulov E. A. Study of dephosphoration and desulphurization processes in the smelting of 20GL steel in the induction crucible furnace with consequent ladle treatment using rare earth metals. *Chernye Metally*. 2017. No. 1. pp. 33–40.
19. Shinkin V. N. Asymmetric three-roller sheet-bending systems in steel-pipe production. *Steel in Translation*. 2017. Vol. 47. No. 4. pp. 235–240.
20. Shinkin V. N. Failure of large-diameter steel pipe with rolling scabs. *Steel in Translation*. 2017. Vol. 47. No. 6. pp. 363–368.
21. Shinkin V. N. Simplified calculation of the bending torques of steel sheet and the roller reaction in a straightening machine. *Steel in Translation*. 2017. Vol. 47. No. 10. pp. 639–644.
22. Lopatenko A. D., Orekhov D. M., Semin A. E. Improving the production of pipe steel. *Steel in Translation*. 2016. Vol. 46. No. 11. pp. 771–775.
23. Zubarev K. A., Kotel'nikov G. I., Titova K. O., Semin A. E., Mikhailov M. A. Predicting the liquidus temperature of complex nickel alloys. *Steel in Translation*. 2016. Vol. 46. No. 9. pp. 633–637.
24. Lim Y., Venugopal R., Ulsoy A. G. Process control for sheet-metal stamping process modeling, controller design and stop-floor implementation. Springer. 2014. 140 p.
25. Lin J., Balint D., Pietrzyk M. Microstructure evolution in metal forming processes. Woodhead Publishing. 2012. 416 p.
26. Belskiy S. M. Parameters of evaluation of shape cross section of hot-rolled steel strips. Message 1. The determination coefficient. *Chernye Metally*. 2017. No. 10. pp. 65–70.
27. Belskiy S. M. Parameters of evaluation of shape cross section of hot-rolled steel strips. Message 2. The saddle coefficient. *Chernye Metally*. 2017. No. 11. pp. 42–47.
28. Qin Y. Micromanufacturing engineering and technology. William Andrew. 2015. 858 p.
29. Hingole R. S. Advances in metal forming. Expert system for metal forming. Springer. 2015. 116 p.
30. Shinkin V. N. Calculation of technological parameters of O-forming press for manufacture of large-diameter steel pipes. *CIS Iron and Steel Review*. 2017. Vol. 13. pp. 33–37.
31. Shinkin V. N. Mathematical model of technological parameters' calculation of flanging press and the formation criterion of corrugation defect of steel sheet's edge. *CIS Iron and Steel Review*. 2017. Vol. 13. pp. 44–47.
32. Predeleanu M., Gilormini P. Advanced methods in materials processing defects. Vol. 45. Elsevier Science, 1997. 422 p.
33. Predeleanu M., Ghosh S. K. Materials processing defects. Vol. 43. Elsevier Science. 1995. 434 p.
34. Lenard J. G. Metal Forming Science and Practice. Elsevier Science. 2002. 378 p.
35. Shinkin V. N. Arithmetical method of calculation of power parameters of 2*N*-roller straightening machine under flattening of steel sheet. *CIS Iron and Steel Review*. 2017. Vol. 14. pp. 22–27.
36. Shinkin V. N. Springback coefficient of the main pipelines' steel large-diameter pipes under elastoplastic bending. *CIS Iron and Steel Review*. 2017. Vol. 14. pp. 28–33.
37. Rees D. Basic engineering plasticity. An introduction with engineering and manufacturing applications. Butterworth-Heinemann. 2006. 528 p.
38. Wilko C. E. Formability. A review of parameters and processes that control, limit or enhance the formability of sheet metal. Springer. 2011. 112 p.
39. Davim J. P. Materials Forming and Machining. Research and Development. Woodhead Publishing. 2015. 202 p.